VDMA
Fluid Power Association

23rd ISC

International Sealing Conference

Stuttgart, Germany
Sept.30 - Oct.1, 2026

Sealing the future –
Facing the challenges of tomorrow

UNI STUTTGART

Fachverband Fluidtechnik im VDMA e. V. Lyoner Str. 18
50628 Frankfurt am Main
Germany

Phone +49 69 6603-1513
E-Mail maximilian.baxmann@vdma.eu

Internet www.vdma.eu/fluid

FEA and Optimization of High-Speed E-Mobility Seal

Barış ENGİN [a], Murat YAZICI [b]

[a] R&D Center, SKT Spare Parts and Machinery Industry and Trade Co., Bursa, Turkey
[b] Bursa Uludag University, Bursa, Turkey

Abstract

The adoption of electric vehicles (EVs) is projected to increase steadily over time. Compared to internal combustion engines, the operating conditions of rotary shaft seals employed in EV powertrains are significantly more demanding. Specifically, these seals must withstand a maximum operating temperature of 150 °C and rotational speeds up to 16,000 RPM. Under such conditions, conventional seals equipped with garter springs are unable to prevent leakage, necessitating the development of alternative design solutions.

The primary objective of this study is to design a next-generation rotary shaft seal for electric vehicles using finite element analysis (FEA) and optimization techniques. The research methodology integrates FEA, optimization algorithms, and geometric design approaches. Initially, an alternative spiral-knurled seal capable of operating at high rotational speeds was developed. Subsequently, the prototype was subjected to lifetime testing.

Experimental results indicated that the first design exhibited approximately 5 g of leakage after seven days of operation. Post-test inspections revealed significant wear, including the removal of spiral features. A finite element model of the initial design was constructed to evaluate radial load performance. Comparison between simulated and experimental radial load values demonstrated a deviation of approximately 4.3%, confirming the accuracy of the Abaqus-based FEA model. The validated model was then optimized within predefined boundary conditions using Isight software. A prototype of the optimized design was manufactured and tested under identical conditions. The optimized seal exhibited approximately 4 g of leakage after 13 days, meeting the customer's lifetime requirement of 10 days. This corresponds to an improvement of approximately 95% in seal durability. In conclusion, a new-generation rotary shaft seal suitable for electric vehicle applications has been successfully developed and validated in accordance with DIN 3761 specifications.

Keywords: Rubber, Rotary Shaft Seal, Friction, Torque Measurement, Sealing Element, Radial Force, Optimization, Abaqus, I-Sight.

1. Introduction

Sealing elements are essential mechanical components used across a broad range of engineering applications, including automotive drivetrains, industrial equipment, gas turbines, and agricultural machinery. Their main purpose is to maintain fluid containment and ensure the integrity of lubrication systems in locations where rotating shafts interact with stationary housings. Furthermore, these components serve as protective barriers against environmental contaminants, thereby reducing wear, preserving lubricant quality, and enhancing the service life of bearings and transmission assemblies.[1], [2], [3] Conventional rotary shaft seals consist of a metallic case, an elastomeric sealing lip, and a garter spring that provides the radial contact force required for sealing. While traditional seal designs are commonly used at rotational speeds up to 8,000 rpm, E-Mobility applications may require reliable operation at speeds approaching 17,000 rpm. Such demanding conditions lead to increased thermal and mechanical loads at the seal-shaft interface, resulting in greater friction, accelerated wear, and a higher risk of leakage. To reduce contact pressure and improve efficiency, the E-Mobility seal investigated in this study was designed without a garter spring. Finite element analysis was employed to evaluate seal behavior and identify an optimized design configuration. Nevertheless, numerical simulations alone are insufficient, and their accuracy must be verified through experimental validation [4], [7], [11], [12],[13]

The numerical analysis of rotary shaft seals presents considerable challenges because elastomer materials exhibit highly nonlinear and large-strain deformation behavior. Accurate simulation of such components often requires substantial computational effort, particularly when three-dimensional finite element models are employed. Hyperelastic constitutive formulations are commonly used to characterize rubber materials, with the Mooney-Rivlin model being one of the most frequently applied approaches in seal engineering. Reliable determination of hyperelastic material parameters depends on experimental characterization of the elastomer. While uniaxial tensile testing provides an initial estimation of material constants, it is generally insufficient for capturing the complete mechanical response of rubber under multi-axial loading conditions. Consequently, biaxial tension, compression, and pure shear tests are often incorporated to obtain a more representative set of material parameters. The combination of nonlinear material behavior, large deformations, and complex shaft-lip contact interactions makes finite element analysis of rotary shaft seals a highly sophisticated engineering problem. [15], [16], [27], [28]

Over the years, extensive research and development efforts have been dedicated to optimizing the design and performance of rotary shaft seals. The objective of optimization is to enhance sealing effectiveness, reduce friction and wear, increase service life, and minimize energy losses. This involves a multidisciplinary approach that considers various factors, including material selection, geometrical configuration, operating conditions, and manufacturing processes.[30], [31]

Optimization methodologies applied to rotary shaft seals encompass both experimental and computational techniques. Experimental studies involve the evaluation of different seal materials, lip designs, and operating parameters through laboratory testing and field trials. These investigations provide valuable insights into the seal performance and help identify opportunities for improvement.[32]

Advanced numerical techniques, including finite element analysis (FEA) and computational fluid dynamics (CFD), play a crucial role in the optimization of rotary shaft sealing systems. FEA is widely employed to assess the mechanical response of seals subjected to various operational conditions, facilitating the evaluation of stress concentrations, contact behavior, deformation mechanisms, and potential failure regions. Meanwhile, CFD serves as a powerful tool for analyzing fluid flow phenomena within the sealing zone, providing valuable information regarding leakage performance, pressure distribution, lubricant transport, and thermal effects. The integration of FEA and CFD enables a comprehensive understanding of seal behavior and supports the development of high-performance sealing solutions with improved durability and efficiency. [32], [33]

Optimization efforts are further supported by advancements in material science and manufacturing technologies. New materials with improved wear resistance, low friction properties, and enhanced chemical compatibility are continuously being developed, allowing for the creation of more effective sealing solutions. Additionally, manufacturing techniques such as precision molding and advanced machining enable the production of seals with tighter tolerances, reduced surface roughness, and improved geometric accuracy.[30], [31], [32]

The optimization of rotary shaft seals is a crucial aspect of improving their performance and reliability. Through a combination of experimental investigations and computational simulations, researchers and engineers can identify and implement design modifications that enhance sealing effectiveness, reduce friction losses, extend service life, and improve overall system efficiency. Continued advancements in materials and manufacturing technologies will further contribute to the development of more efficient and durable rotary shaft seals.[30], [31], [33]

There are two main categories of methods for addressing conceptual design optimization: gradient-based methods and non-gradient-based methods, such as metaheuristics. These methods have distinct advantages and disadvantages. Gradient-based methods typically exhibit rapid convergence rates, but they are limited in their ability to handle problems where derivative functions are unavailable or when the design variables are discrete. On the other hand, although metaheuristics are slower, they offer the advantage of being derivative-free and highly adaptable. They can effectively address black-box optimization problems and are particularly well-suited for aircraft conceptual design optimization due to the presence of discrete variables like airfoil profiles and engine models. Moreover, metaheuristics excel in solving multi-objective optimization problems and can generate a Pareto front in a single optimization run.[34]

Metaheuristics can be classified into single-objective and multi-objective optimization, with many-objective optimization referring to the special cases involving more than three objective functions. Over time, metaheuristics have undergone continuous development. Initially, the focus was on single-objective design, with popular algorithms such as Genetic Algorithms (GA), Differential Evolution (DE), and Particle Swarm Optimization (PSO) being widely used. Since then, numerous algorithms have been developed, drawing inspiration from various sources such as animal behavior (e.g., Artificial Bee Colony algorithm, Ray Optimization, Dolphin Echolocation, Moth-Flame Optimization, Dragonfly Algorithm, Whale Optimization, Crow Search Algorithm, Salp Swarm Algorithm, Symbiotic

Organisms Search) as well as nature or physics (e.g., Water Cycle Algorithm, Multi-verse Optimizer, Water Evaporation Optimization, Vibrating Particle System, Henry Gas Solubility Optimization, Equilibrium Optimizer). Additionally, metaheuristics have been enhanced by incorporating adaptive strategies, hybrid algorithms, and other complementary methods.[35], [36], [37]

In the realm of multi-objective optimization, there are several well-known and recently developed algorithms that have gained recognition. These include the Fast and Elitist Multi-Objective Genetic Algorithm (NSGA-II), Differential Evolution for Multi-Objective Optimization (DEMO), Multi-Objective Cuckoo Search Algorithm (MOCS), Multi-Objective Slime Mould Algorithm (MOSMA), Multi-Objective Jellyfish Search Algorithm (MOJS), Multi-Objective Evolutionary Algorithm based on Decomposition (MOEA/D), Multi-Objective Bat Algorithm with Non-Dominated Sorting (MOBANS), Multi-Objective Flower Pollination Algorithm (MOFPA), Artificial Immune System, Two Archive Algorithm, Multi-Objective Gray Wolf Optimizer, Multi-Objective Ant Lion Optimizer, and Multi-Objective Multi-Verse Algorithm (MOMVO). These multi-objective algorithms are generally well-suited for addressing many-objective optimization problems. Additionally, there are specific algorithms designed to tackle the complexities of many-objective problems, such as the Preference-Inspired Coevolutionary Algorithm, An Improved Two Archive Algorithm (Two Arch2), Knee Point-Driven Evolutionary Algorithm for Many-Objective Optimization (KnEA), Reference Vector Guided Evolutionary Algorithm (RVEA), Many-Objective Nondominated Sorting Genetic Algorithm (NSGA-III), and Self-Adaptive Many-Objective Metaheuristic based on Decomposition (A-MnOMH/D).[38], [40], [41]

2. Materials and Method

2.1 Product Design

Standard rotary shaft seals consist of three different semi-components. These components are metal ring, elastomer material and garter spring. Elastomer material type is changing according to rotary shaft seal operating conditions. Garter spring's function is to provide proper contact pressure between shaft and seal lip. When the seal rotates, the heat generation caused by friction torque occurs and lip temperature increases according to Rpm.

The contact pressures of the seals using spring are higher than the seals without garter spring. High contact pressures cause high temperature rise in the lips. High lip temperature causes leakage.

Operating conditions for E-mobility seal is:

Bore Diameter: 70 mm

Bore Depth:9 mm

Shaft Diameter:45mm

Max. Velocity: 17.000 Rpm

Max. Oil Temperature:150 °C

According to design criteria, alternative spiral knurled(E-Mobility) seal was designed by SKT R&D Team. The section of E-Mobility seal was shown Figure 1-a.

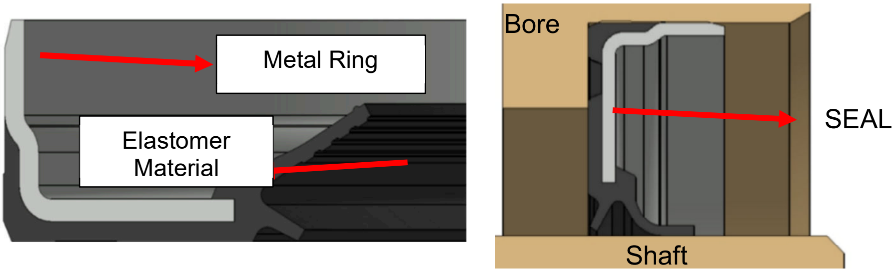

Figure 1. E-Mobility Seal Section (a) Assembled Section (b)

Elastomer material type FPM was selected from operating conditions as shown Figure 2.

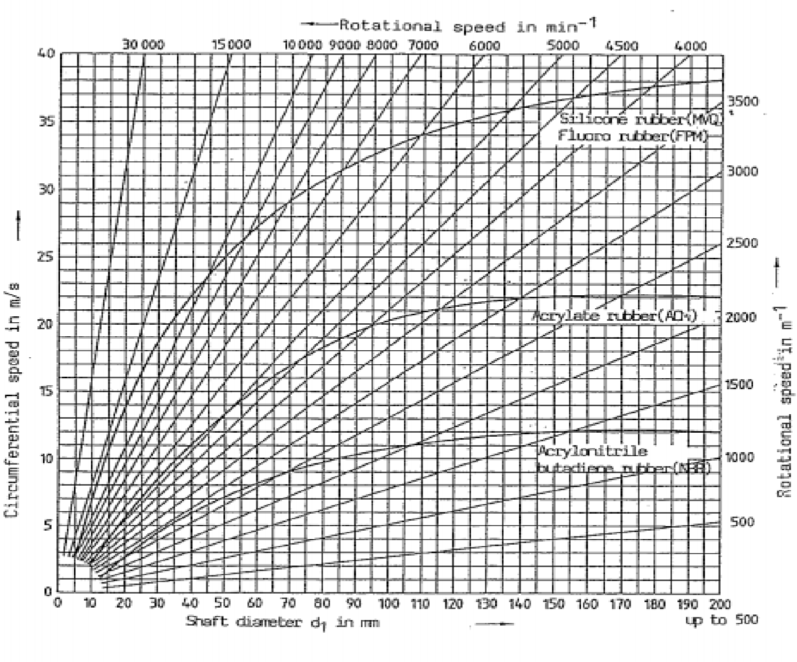

Figure 2. Material Selection Graph (DIN 3761)

2.2 *Finite Element Analysis*

Radial load and contact pressure are the most important parameters to prevent leakage. For this reason 2D axisymmetric FEA model was occurred. The reason why axisymmetric 2D FEA model used is the less solution time. In this study we used ABAQUS 2020 which gives the best solution for nonlinear hyperelastic analyses. Firstly, semi-components of E-mobility seal were designed on Abaqus 2020 as shown Figure 3.

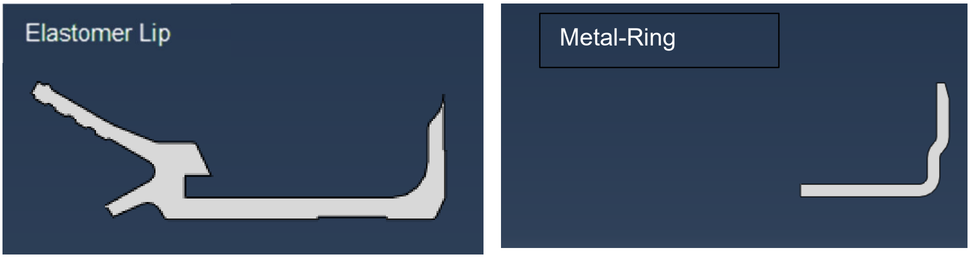

Figure 3. Semi Components of E-Mobility (a)Elastomer Lip (b) Metal Ring

After the design of semi components, material informations were defined. Steel which used for metal ring was defined according to data sheet. Some tests were needed to find Mooney Rivlin coefficient for Rubber material. Unaxial tensile test, bi-axial tensile test and compression test (Figure 4) were done to find the nearest Mooney Rivlin coefficient. Result graphs for Unaxial tensile test, bi-axial tensile test and compression test were shown Graph 1, Graph 2 and Graph 3.

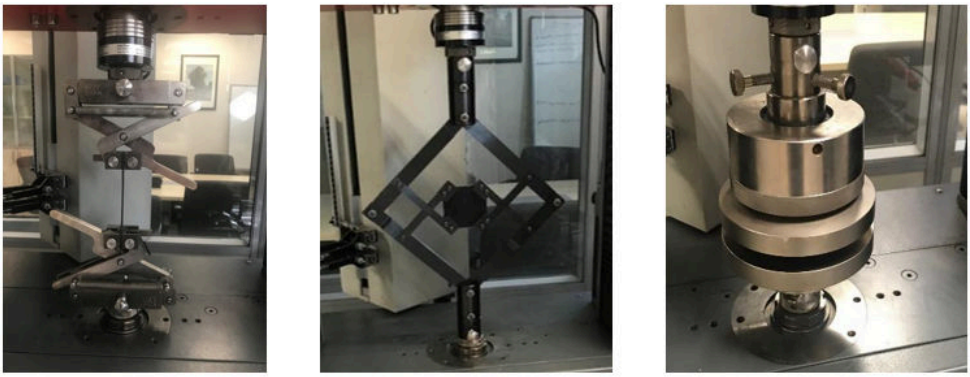

Figure 4. Tests (a) Uniaxial Tensile (b) Biaxial Tensile (c) Compression

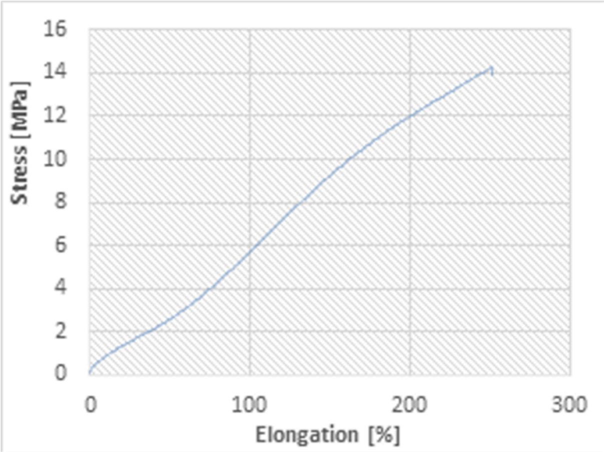

Graph 1. Uniaxial Tensile

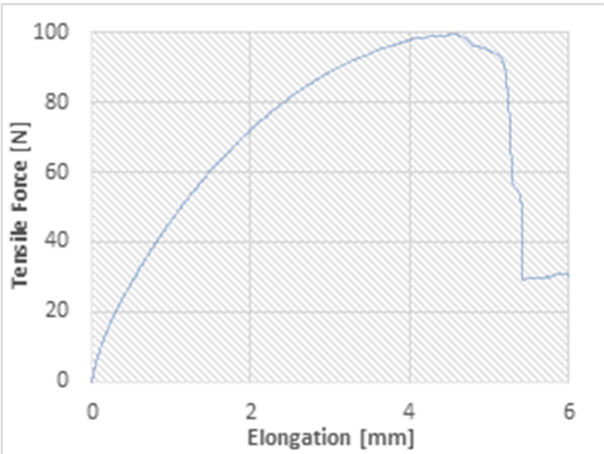

Graph 2. Biaxial Tensile

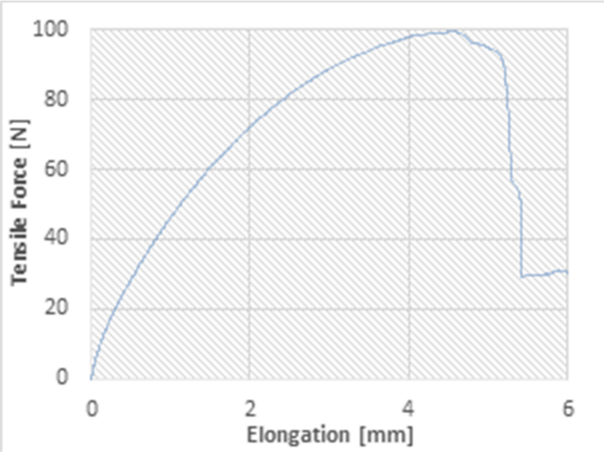

Graph 3. Compression

Mooney Rivlin coefficients for FPM material as shown Table 1 were calculated according to test results.

Table 1. Mooney Rivlin Coefficient

C10	C01	D1
0.47	2.15	0

After entering material coefficients from data sheet and tests, assembly design was completed as shown Figure 5.

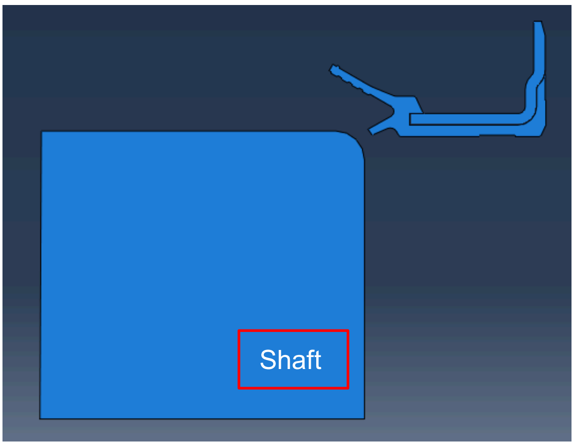

Figure 5. Assembly Design

After the assembly design, interaction informations were defined. Tie contact was defined between metal ring and elastomer lip as shown Figure 6-A. Surface to surface interaction was defined between shaft and elastomer lip as shown Figure 6-B.

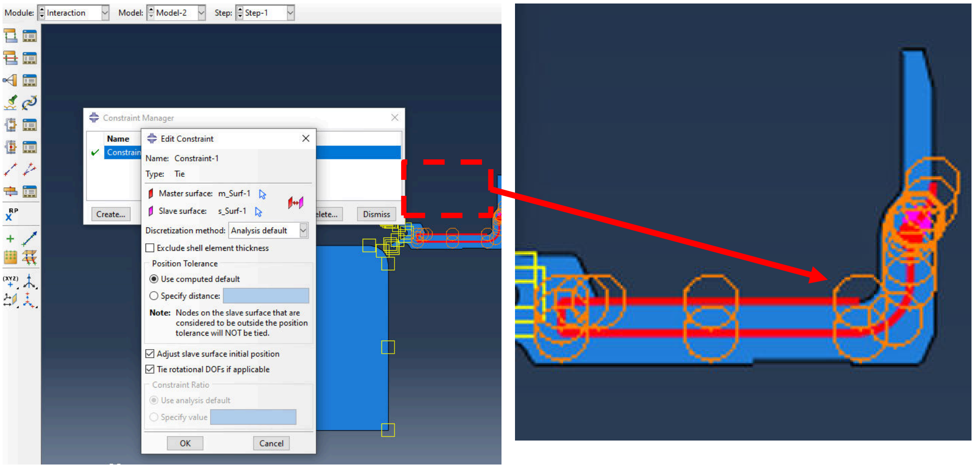

Figure 6. Interactions (a) Tie Contact

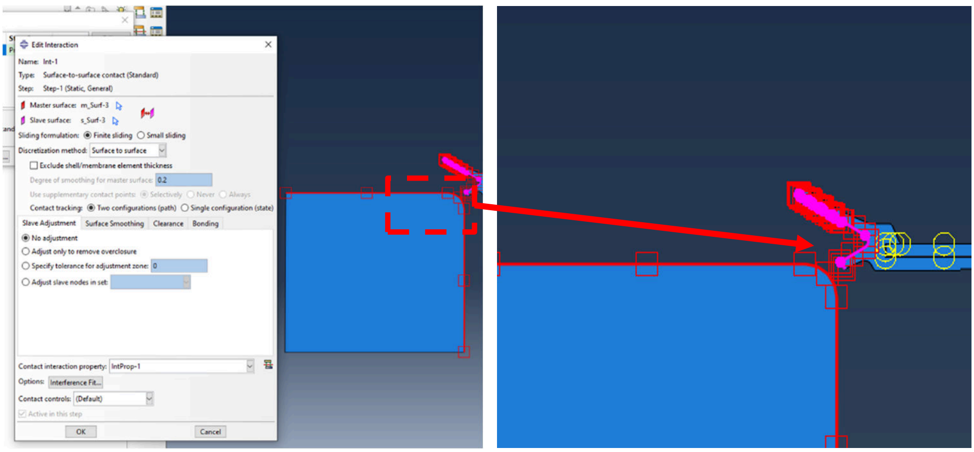

Figure 6. Interactions (b) Surface-Surface

After the assembly design, mesh structure was created according to 2D axisymmetric model as shown Figure 7. Mesh structure of E-Mobility seal was created from 14.357 number CAX4H type mesh elements and 438 number CAX3H type mesh elements.

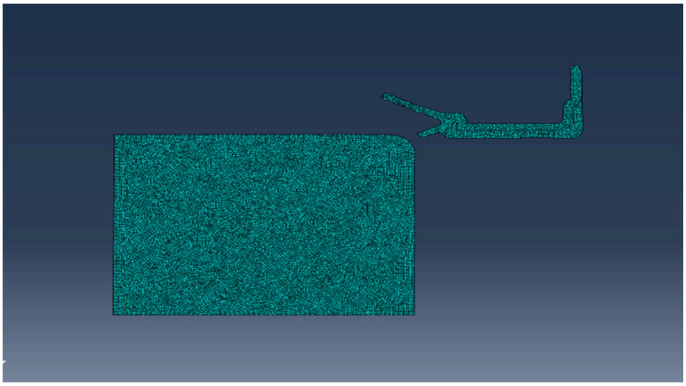

Figure 7. Mesh Structure

After creating mesh structure, analyses job was created and submitted. The results taken from FEA was similar to experimental results. Contact length result taken from FEA was approximately 1.4 mm as shown Figure 8.

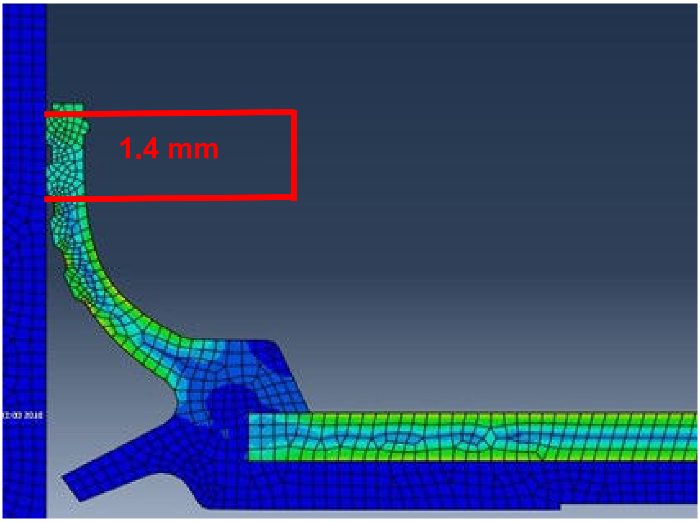

Figure 8. Contact Length

When the seal is mounted on housing and shaft, lip position on shaft is one of the most important parameter to check spiral number.

2.3 Protype Manufacturing

Finite Element Analyses results are not meanless unless supported with experimental results. For that reason, metal ring and vulcanization molds are designed and manufactured as shown Figure 9.

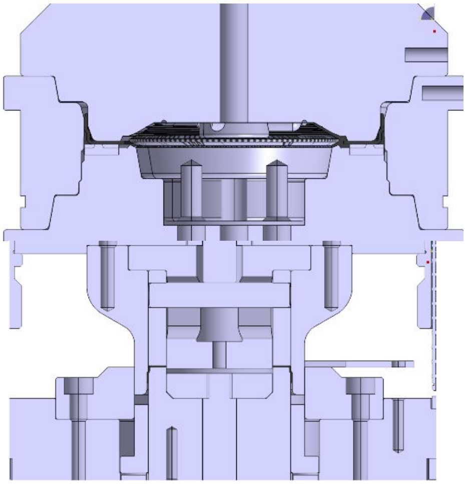

Figure 9. Mold Designs (a) Vulcanization Mold (b) Metal Ring Mold

After the mold productions, preforms of E-mobility seal were prepared as shown Figure 10.

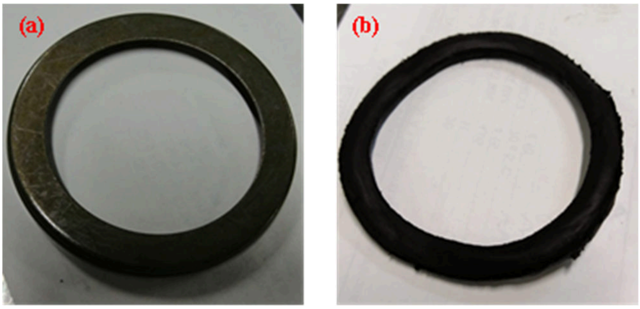

Figure 10. Preforms (a) Metal Ring (b) Elastomer Preform

After preforms of E-mobility seal were produced, protype seals were manufactured (Figure 11-a), measured with Nikon iNEXIV VMA-2520 and prepared measurement report results were shown Table 2.

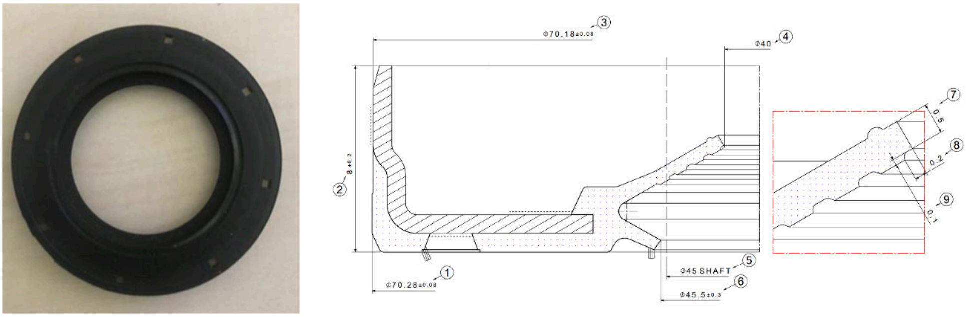

Figure 11. Prototype Manufacturing (a) Prototype Seal (b) Technical Drawing

Seal dimensions were checked according to technical drawing as shown Table 2.

Table 2. Dimensional Report

Dimension No	Dimension From Technical Drawing	Measured Value from Prototype Part	Status
1	Ø70.28 ± 0.08	Ø70.33	OK
2	Ø70.18 ± 0.08	Ø70.24	OK
3	8 ± 0.2	7.97	OK
4	Ø40 ± 0.2	Ø39.86	OK
6	Ø45.5 ± 0.3	Ø45.56	OK
7	0.5 ± 0.2	0.65	OK
8	0.2 ± 0.1	0.18	OK
9	0.1 ± 0.05	0.08	OK

One of the most important parameters to check functionality of rotary shaft seal is Radial Load. Seal performance depends upon the sealing force or radial load that the seal lip exerts on the shaft after installation. The force can be estimated by measuring the lip opening pressure (LOP). The LOP is defined as the amount of pressure applied to the air side of the seal that will lift the lip and allow 10,000 cm3/min of air to pass under the lip. This measurement is widely used in industry as a quality check on production parts. It is loosely related to radial load, but a direct correlation from one seal design to another is not possible since the LOP is dependent upon seal geometry as well as on the radial load. Radial load method is defined within DIN 3761-8. Radial load measurement of E-mobility seals were done with Radial Load Device (SKT, Turkey). (Figure 12)

Figure 12. Radial Load Measurement

2.4. Comparison Of FEA Results and Experimental Results

FEA is meanless unless experimental results compared with FEA results. For that reason, experimental results of E-Mobility seal were compared with FEA results and comparison table shown below.

Table 3. Results Comparison

	Spiral Number on Contact	Contact Length (mm)	Radial Load (N)
Experimental	2	1.43	7
FEA	2	1.4	7.2

FEA results and Experimental results were similar as shown Table 1. Axial cut-off molds designed according to DIN 3761-8 are used to check this situation. After the axial cut-off mold for E-mobility seal was produced, E-mobility seal section was trimmed as shown Figure 13. After checking results validation test machine design and validation study were started.

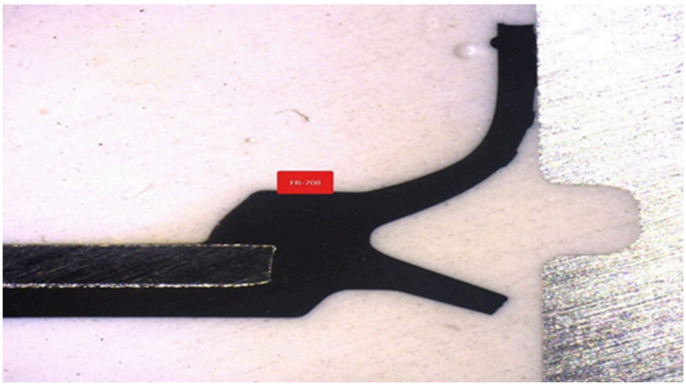

Figure 13. E-Mobility Seal Section

E-Mobility seal section was measured with digital microscope ZEISS Smartzoom 5 and contact length of lip was 1.43 mm.

2.5. Functional Test and Test Machine Design

High speed functional test device as shown Figure 14 was developed and manufactured by EMSA&SKT Cooperation. High speed functional test device's specialities are:

- Max. 24.000 Rpm
- Continous Lip Temperature Measurement
- Continous Torque Measurement
- Operating Temperature : 60 – 180 º C
- Indirect Heating & Cooling

Figure 14. High Speed Functional Test Device

Six first generation E-mobility seals were tested on High Speed Functional Test Device according to E-Mobility Car Manufacturers' test conditions. Test Conditions taken from E-Mobility Car Manufacturers are:

- Max. rotation velocity: 16.000 Rpm
- Max. operating temperature: 150°C
- Oil Type : Shell 75W

At end of 7 days leakage occurred all tests for first generation E-Mobility seal as shown Figure 15. After the test six first generation E-mobility seal were investigated and test reports were created.

TEST PROGRAMS						
Step No	Step Duration (min)	Temperature (± 3 ºC)	Rotation per min. (rpm)	Velocity (m/s)	Shaft Rotating Direction	Cycle Number (Days)
1	600	110	8000	18,8	Right	10
2	360	110	10000	23,6	Right	10
3	180	130	13000	30,6	Right	10
4	60	130	16000	37,7	Right	10
5	240	23	0	0,0		10

Total Duration of Steps (min)	1440	Total Cycle	10	Targeted Total Work (Min/Hour/Day)	14400	240	10

TESTS PROPERTIES (BEFORE AND AFTER)				
PROPERTIES	BEFORE	AFTER	PROPERTIES	AFTER
Internal Dia. without spring (mm)	39,86	44,53	Friction Surface Width (mm)	0,1
Internal Dia with spring (mm)			The crack at lip (Yes / No)	NO
2. Internal Dia. without spring (mm)			Is contact patern correct (Yes / No)	NO
2. Internal Dia with spring (mm)			Lip Hardening (Yes / No)	NO
Protective Lip Internal Dia. (mm)	45,56	45,75	Leakage oil quantity (g)	5,07 Gr.
Rubber Outer Dia. (mm)	70,33	70,15	Leakage from test slot (g)	0,0 Gr.
Metal Outer Dia. (mm)	70,24	70,08	Permanent Deformation in Dia – w/o Spring (%)	10,49%
Ovality	0,02/0,02	0,02/0,03	Permanent Deformation in Dia – with Spring (%)	
Coaxiality of seal lip acc. to external dia.	0,08	0,07	Carbonization on lips (Yes / No)	NO

ADDITIONAL RESULTS AND EVALUATIONS		
* At the end of 7 days 5 gr leakage.		
Result		
Test Operator	Results (OK / NOK)	APPROVAL

Figure 15. Test Report Example

Approximately 5 g leakage occurred at the end of 7 days according to test reports. Another important detail from test reports that some spirals on lip was effaced as shown Figure 16. This means that radial load for first generation E-mobility seal was high so optimization of first generation E-Mobility seal was needed.

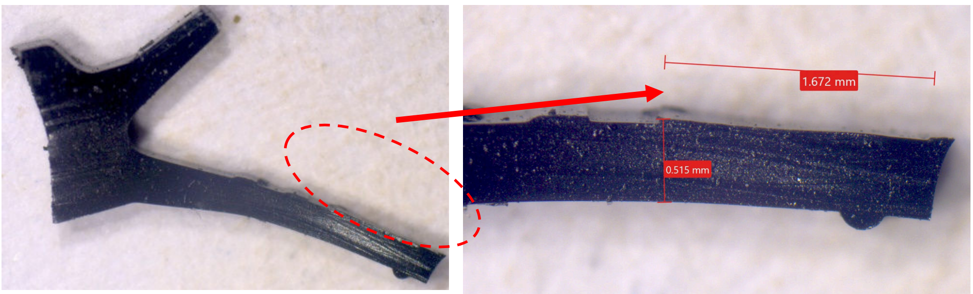

Figure 16. Effaced Spirals

2.6 I-Sight Optimization

Before FEA model which was created for first generation of E-mobility seal, optimization situation was not thought. For that reason, parametric lip sketch was (Figure 17-a) created and FEA job was also worked All needed files for optimization on I-sight program were ready and boundary conditions for parametric lip were determined. After the determination of boundary conditions, an objective function for radial load minimization was created as shown Table 4.

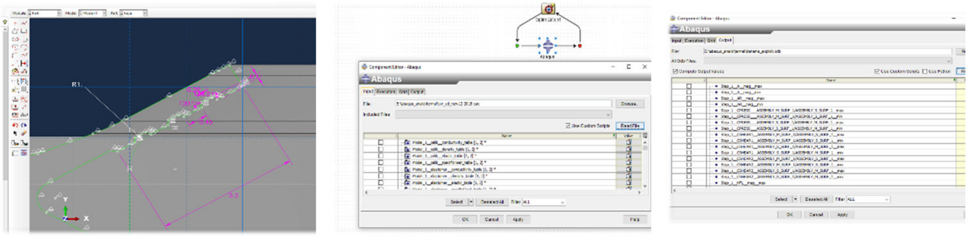

Figure 17. I-Sight Screenshots (a) Parametric Lip Model (b) Input Parameters (c) Output Parameters

Table 4. Optimization Parameter

Boundary Conditions	Objective Function	Results
0,30 < Dimension 7 <0,70		Dimension 7 = 0,41
0,10 < Dimension 8 <0,30	Minimize Total Contact Force on Seal Lip	Dimension 8 = 0,30
0,05 < Dimension 9 < 0,15		Dimension 9 = 0,11

The Hooke-Jeeves algorithm is chosen with most options left at the default values and the output parameter CFT selected as the goal with a target of 0.01 as shown Figure 18.

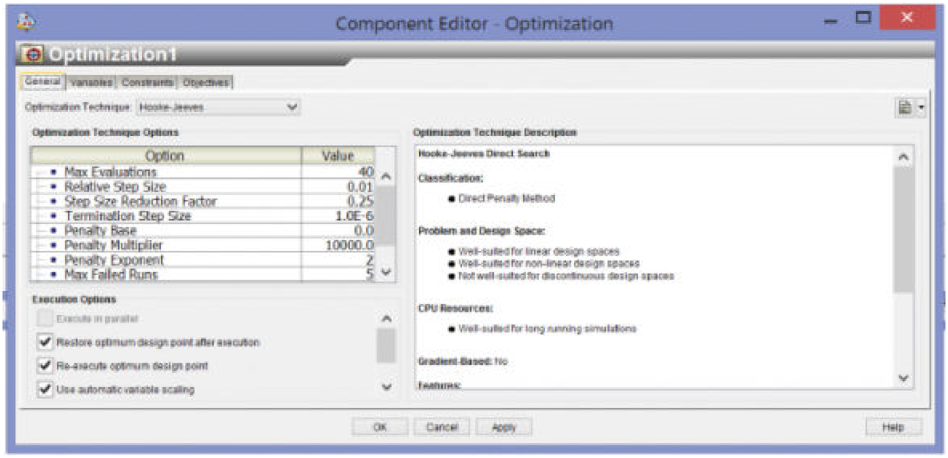

Figure 18. Hooke-Jeeves Method

The Hooke-Jeeves algorithm, also known as “pattern search” s a family of numerical optimization methods that does not require a gradient. As a result, it can be used on functions that are not continuous or differentiable. One such pattern search method is "convergence" (see below), which is based on the theory of positive bases.

Optimization attempts to find the best match (the solution that has the lowest error value) in a multidimensional analysis space of possibilities.

In light of this information I-sight model was worked, the results were taken. The lip form was updated according to I-Sight result as shown Table 4.

Second generation of E-Mobility Seal was designed and vulcanization mold of first generation of E-Mobility Seal was updated. After the vulcanization mold update, all preforms for second generation of E-Mobility Seal were prepared and prototypes of second generation E-Mobility Seal was produced. All revised dimensions on seal lip were checked and confirmed as shown Table 5.

Table 5. Optimized Prototype Part Measurement

Dimension No	Measured Value from Optimized Prototype Part	Status
1	Ø70.30	OK
2	Ø70.22	OK
3	7.93	OK
4	Ø39.95	OK
6	Ø45.76	OK
7	0.40	OK
8	0.30	OK
9	0.11	OK

After the dimensional check, radial load for second generation of E-Mobility Seal was measured and the value is 5 N. When the radial load comparison was made, 28% reduction in radial load was seen.

2.7 Functional Test for Second Generation E-Mobility Seal

Functional tests for second generation E-Mobility Seal were done according to E-Mobility Car Manufacturers' test conditions. Second generation E-Mobility Seal had approximately 4 g of leakage after 13 days under the same test conditions like first generation Seal. After finishing functional tests, investigations of seal lip were completed and any wear on second generation E-Mobility Seal was not found as shown Figure 19.

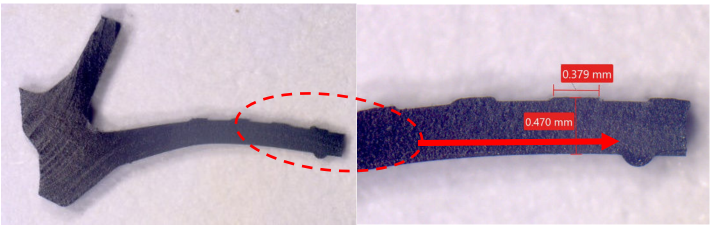

Figure 19. Spirals without wear

3. Conclusion

The use of electric vehicles is expected to increase day by day. The operating conditions of the rotary shaft seals used in the powertrain of electric vehicles are more challenging than those of internal combustion engines. For that reason a new type seal design study was started and good results were taken from new type seal design. The important results are shown below:

- New generation FPM material recipe was developed
- New type seal design was developed
- Test Conditions for E-Mobility Seal was determined
- Optimization study was done according to first generation E-Mobility Seal. After the revision of design according to optimization, 28% reduction in radial load was seen.
- The lower radial load on seal the lower wear on spirals
- Although 28% reduction in radial load was seen, the lifetime of the seal was approximately 95% improved.

4. Acknowledgement

This work was funded by SKT Spare Parts Co. and Bursa Uludağ University. The author would like to thank the staff for providing the use of composite samples and test equipment necessary for the experiments.

5. Declaration of Conflicting

The authors declare that there are no financial contributions or other potential (potential) conflicts of interest that should be known about the objectivity of the study and the area of the relationship.

6. REFERENCES

[1] Burkhart C, Weyrich D, Thielen S, Schollmayer T, Sauer B. Development and Optimization of a Tribometer for Radial Shaft Seals. *ASME Journal of Tribol*ogy *2021*; 143(4): 041201. https://doi.org/10.1115/1.4049597

[2] Johnston, D.E., Bond, R. (1984). A new concept in rotary shaft seal design suitable for truck and bus hub seal applications. SAE Technical Papers, 93(May), 1081–1091.

[3] Bien-aimé, L. K. M., Blaise, B. B., Beda, T. (2020). Characterization of hyperelastic deformation behavior of rubber-like materials. SN Applied Sciences, 2(4).

[4] Kim, B., Lee, S. B., Lee, J., Cho, S., Park, H., Yeom, S., Park, S.H. (2012). A comparison among Neo-Hookean model, Mooney-Rivlin model, and

Ogden model for Chloroprene rubber. International Journal of Precision Engineering and Manufacturing, 13(5), 759–764.

[5] Bhandari, A., Erdman, D., Bhatia, A., Strang, W. (2007). Finite Element Analysis and Material Modeling of Elastomeric Components and Assemblies: Some Practical Considerations. In SAE Technical Papers (Vol. 2007- January). SAE International.

[6] Li, W., Mays, S., Lam, D. (2002). Material and finite element analysis of poly(tetrafluoroethylene) rotary seals. Plastics, Rubber and Composites, 31(8), 359–363.

[7] Zhang, F. Y., Chen, J. L., Li, T. T., Zhang, Y. F. (2019). Study and Optimization of Structural Parameters of Oil Seal by Response Surface Method. International Journal of Precision Engineering and Manufacturing, 20(2), 255–265.

[8] Starostin, N.P., Vasileva, M.A. (2020). Determination of Load- Speed Modes for Fluoroplastic Seals of Rotary Shaft by Temperature Limitation. IOP Conference Series: Earth and Environmental Science, 459(6).

[9] Zhou, S. M., Chen, P., Shi, Y. (2015). Analysis on Sealing Performance for a New Type of Rubber Saddle-shaped Sealing Ring Based on AQAQUS. In Procedia Engineering (Vol. 130, pp. 1000–1009). Elsevier Ltd.

[10] Calonius, O., Pietola, M. (2005). Explicit Finite Element Analysis of Tracking Capability of Rotary Face Seal for Industrial Fluid Power Applications. Proceedings of the JFPS International Symposium on Fluid Power, 2005(6), 328–333.

[11] Azura, A.R., Leow, S.L. (2019). Effect of carbon black loading on mechanical, conductivity and ageing properties of Natural Rubber composites. In Materials Today: Proceedings (Vol. 17, pp. 1056–1063). Elsevier Ltd.

[12] Li, H., Zhao, T., Chen, M. (2016). Green tire and new type rubber materials. Kexue Tongbao/Chinese Science Bulletin, 61(31), 3297–3303.

[13] Vahapoğlu, V. (2013). Kauçuk Mekaniğinde Yapılan Deneyler . Pamukkale Üniversitesi Mühendislik Bilimleri Dergisi , 19 (1) , 33-60 .

[14] Keerthiwansa, R., Javorik, J., Kledrowetz, J., Nekoksa, P. (2018). Elastomer testing: The risk of using only uniaxial data for fitting the Mooney-Rivlin hyperelastic-material model. Materiali in Tehnologije, 52(1), 3–8.

[15] Dalrymple, T., Choi, J., Miller, K. (2007). Elastomer rate- dependence: a testing and material modelling methodology. Meeting of the Rubber Division

of , (October 2007). Retrieved from Abdullah, M.A. (2020). Fundamental Considerations for Finite Element Modelling of Rubber Material Tensile Test. International Journal of Engineering and Management Sciences, 5(2), 7–13.

[16] Sasso, M., Palmieri, G., Chiappini, G., Amodio, D. (2008). Characterization of hyperelastic rubber-like materials by biaxial and uniaxial stretching tests based on optical methods. Polymer Testing, 27(8), 995–1004.

[17] Freitas, T.R. (2009). Rubber sealing study applied to ball bearing components using finite element method. In SAE Technical Papers. SAE International.

[18] Erkek, M., Kaya, N., Güven, C. (2015). Kauçuk Burçların Hiperelastik Modellenmesi ve Sonlu Elemanlar Yöntemi ile Analizi . Uludağ University Journal of The Faculty of Engineering , 20 (1) , 65-74 . Retrieved from Fujikawa, M., Maeda, N., Yamabe, J., Kodama, Y., Koishi, M. (2014). Determining Stress–Strain in Rubber with In-Plane Biaxial Tensile Tester. Experimental Mechanics, 54(9), 1639–1649.

[19] Kanzenbach, L., Schlomka, C., Gelke, S., & Ihlemann, J. (2019). Specimen design for extreme uniaxial tension-compression tests of rubber materials. PAMM, 19(1).

[20] Huri, D., Mankovits, T. (2018). Comparison of the material models in rubber finite element analysis. In IOP Conference Series: Materials Science and Engineering (Vol. 393). Institute of Physics Publishing.

[21] Xu, D., Han, B. H., He, W. H., Cheng, Z. G. (2018). Research on compressive mechanical properties of metal rubber and its constitutive relation model. Journal of Vibroengineering, 20(1), 332–344.

[22] Ismail, R., Ibrahim, A., Rusop, M., Adnan, A. (2018). Determination of mechanical properties natural rubber compounds using double shear test pieces. International Journal of Civil Engineering and Technology, 9(8), 37–43.

[23] Soltani, A., Deng, A., Taheri, A., Mirzababaei, M., Nikraz, H. (2019). Interfacial shear strength of rubber-reinforced clays: A dimensional analysis perspective. Geosynthetics International, 26(2), 164–183.

[24] Yang, Y., Ren, Z. Y., Bai, H., Shen, D., Zhang, B. (2020). Study on the Mechanical Properties of Metal Rubber Inner Core of O-Type Seal with Large Ring-to-Diameter Ratio. Advances in Materials Science and Engineering, 2020.

[25] Yakovlev, S.N. (2019). An Experimental Study of the Wear of the Radial Shaft Seals of Rotary Shafts. Journal of Machinery Manufacture and Reliability, 48(2), 179–183.

[26] Kumar, N., Rao, V. V. (2016). Hyperelastic Mooney-Rivlin Model : Determination and Physical Interpretation of Material Constants. MIT International Journal of Mechanical Engineering, 6(1), 43–46.

[27] Kim, B., Lee, S. B., Lee, J., Cho, S., Park, H., Yeom, S., Park, S.H. (2012). A comparison among Neo-Hookean model, Mooney-Rivlin model, and Ogden model for Chloroprene rubber. International Journal of Precision Engineering and Manufacturing, 13(5), 759–764.

[28] Engin, B., Saraç, Yazıcı, M. (2019). Finite element simulation of rotary shaft lip seals. Acta Physica Polonica A, 135(5), 1072– 1074.

[29] Zhou, Y., Huang, Z., Tan, L., Ma, Y., Qiu, C., Zhang, F., Yuan, Y., Sun, C., Guo, L. (2014). Cone bit bearing seal failure analysis based on the finite element analysis. Engineering Failure Analysis, 45, 292–299.

[30] Jones, W. J. (2012). Rotary shaft seals: A guide to sealing principles, materials, designs, and applications. John Wiley & Sons.

[31] Iliev, O., Borisov, S., Bontchev, B., & Gabrovski, M. (2016). Design optimization of rotary shaft seals. Journal of Theoretical and Applied Mechanics, 46(3), 17-32.

[32] Qiu, Y., Tian, Y., & Luo, X. (2018). Multi-objective optimization of lip seal based on fluid-structure interaction analysis. Tribology International, 122, 70-79.

[33] Karasek, R. (2019). Rotary Shaft Seals Optimization in Hydropower Machinery. In Proceedings of the 7th World Congress on Mechanical, Chemical, and Material Engineering (MCM'19).

[34] Wang H, Jiao L, Yao X (2015) Two Arch2: an Improved two- archive Algorithm for many-objective optimization. IEEE Trans Evol Comput 19(4). https://doi.org/10.1109/TEVC.2014.2350987

[35] Zhang X, Tian Y, Jin Y (2015) A knee point-driven evolution- ary algorithm for many-objective optimization. IEEE Trans Evol Comput 19(6). https://doi.org/10.1109/TEVC.2014.2378512

[36] Cheng R, Jin Y, Olhofer M, Sendhoff B (2016) A reference vec- tor guided evolutionary algorithm for many-objective optimiza- tion. IEEE Trans Evol Comput 20(5). https://doi.org/10.1109/ TEVC.2016.2519378

[37] Deb K, Jain H (2014) An evolutionary many-objective optimi- zation algorithm using reference-point-based nondominated sorting approach, part I: solving problems with box constraints. IEEE Trans Evol Comput 18(4). https://doi.org/10.1109/ TEVC.2013.2281535

[38] Champasak P, Panagant N, Pholdee N, Bureerat S, Yildiz AR (2020) Self-adaptive many-objective meta-heuristic based ondecomposition for many-objective conceptual design of a fixed wing unmanned aerial vehicle. Aerosp Sci Technol 100. https:// doi.org/10.1016/j.ast.2020.105783

[39] Zeng C, Abnous R, Gabani K, Chowdhury S, Maldonado V (2020) A new tilt-arm transitioning unmanned aerial vehicle: introduction and conceptual design. Aerosp Sci Technol 99. https://doi.org/10.1016/j.ast.2020.105755

[40] CHAI X, X. YU, and, WANG Y (2018) Multipoint optimization on fuel efficiency in conceptual design of wide-body aircraft. Chin J Aeronaut 31(1). https://doi.org/10.1016/j.cja.2017.10.006

[41] Singh V, Sharma SK, Vaibhav S (2016) "Transport Aircraft Conceptual Design Optimization Using Real Coded Genetic Algorithm," International Journal of Aerospace Engineering, vol. 2016, doi: https://doi.org/10.1155[2016]2813541

[42] Silva HL et al (2021) A multidisciplinary design optimization for conceptual design of hybrid-electric aircraft. Struct Multidisci- plinary Optim 64(6). https://doi.org/10.1007/s00158-021-03033-8

https://doi.org/10.61319/XUVJST6A